ACSES *proceedings*

2008

Three-Dimensional Modeling of Receiver Functions in the Peninsular Ranges and Gulf Extensional Province

Christopher Lynch

CSRC an interdisciplinary gateway to the future

San Diego State University

Three-Dimensional Modeling of Receiver Functions in the Peninsular Ranges and Gulf Extensional Province

Christopher Lynch

Knowledge of the Earth's crustal structure is critical for estimating seismic hazards, for resource exploration, and for understanding the dynamic processes that shape the Earth. Receiver function analysis of seismic body wave data can be used to discern the geological structure under a seismic receiving station [e.g., *Langston*, 1979; *Owens et al*., 1984; *Ammon et al*., 1990, 1991, *Reading and Kennett*, 2003]. Receiver function analysis of passive (i.e., from earthquakes) teleseismic data is an important method used to estimate the thickness of Earth's crust in the vicinity of individual seismic stations [*Langston and Hammer,* 2001]. Teleseismic data is seismic data that is recorded at epicentral distances equal to or greater than 3,335 km ($\Delta \geq 30^o$) and is especially useful in providing such estimates.

Estimates of the distance from the Earth's surface to the Mohorovičić seismic discontinuity (Moho) are good approximations of the thickness of the Earth's crust. The Moho is the compositional and rheological boundary between the Earth's lower crust and upper mantle. This boundary often exhibits a marked decrease in seismic wave speed from that of the dense upper mantle material to the less dense lower crustal material. The sharp velocity contrast (impedance) at this structural boundary causes a portion of the incident seismic energy to be reflected while allowing the remainder to be transmitted through (refracted). Another effect that is produced when a seismic wave is obliquely incident upon such a boundary is the conversion of a portion of the wave energy from one wave type to another, i.e., an incident P wave (or S wave) will produce reflected P (compressional waves) and S waves (shear waves) as well as transmitted P and S waves [*Stein and Wysession,* 2003].

Receiver function analysis is primarily used to isolate and enhance the direct mantle P wave and the converted S wave (Ps) generated at the crust-mantle boundary. Because P and S waves travel at different speeds, the difference in arrival times between the P phase and the converted S phase can be used to estimate the depth to the Moho given an estimate of the seismic velocities under a seismic receiver station [e.g., *Langston*, 1979; *Owens et al*., 1984; *Ammon et al*., 1990]. The receiver function method provides point estimates of Moho depth [*Zhu and Kanamori*, 2000]. Teleseismic receiver functions can provide information about the structure of the lithosphere and upper mantle on a regional scale. Their resolution is greater than that of earthquake tomography, but is less than that of active source seismic reflection and refraction surveys. However, active source surveys require large explosive sources capable of generating energy sufficient to sample that deeply in the Earth, and so tend to be quite costly [*Zhu and Kanamori*, 2000, *Reading and Kennett*, 2003].

There is always a level of uncertainty associated with each model whether it is a structural or a velocity model due to the nonuniqueness inherent in geophysical modeling [*Ammon et al.,* 1990*, Langston and Hammer,* 2001]. That is, there is usually more than one model, and often many more, that will yield synthetic data which will fit the observed data about as well. For this reason it is necessary to consider additional information to help identify the more probable geological model(s) that describe the geologic structure of the region of interest. The results from other types of geophysical investigations such as gravity or geomagnetic surveys can provide additional constraints [e.g., *Jones & Phinney*, 1998]. Additionally, by employing different types of seismic data analysis and modeling techniques, the number of probable models can be further reduced and will be better constrained [e.g., *Langston and Hammer,* 2001]. Theoretical waveform modeling is one of the most useful tools for interpreting observed seismograms and refining the Earth structure models inferred from them [*Lay and Wallace*, 1995]. To aid the interpretation of receiver functions (RF's) theoretical synthetic seismograms are generated for geophysical models of proposed geological structures. If a receiver function produced from a synthetic seismogram generated for a proposed geological Earth model closely matches the receiver function produced from the observed data then confidence in the proposed geological model is increased [*Langston*, 1979].

Most conventional receiver function modeling assumes a flat planar Moho and does not include effects due to 3D structure [*Ammon*, 2001]. However, some studies have directly addressed how 3D dipping structures affect receiver functions [e.g., *Zhang and Langston*, 1995]. These have established the techniques and criteria for identifying such complex interface geometries. The forward modeling used to constrain the effects of dipping structure in previous investigations has usually been done using various ray-tracing or spectral methods. The use of a 3D elastodynamic finite difference modeling technique to investigate these effects contributes additional information using an independent method.

The purpose of this study is to investigate seismic waveforms resulting from sub-vertical incidence of teleseismic P waves on dipping and other complex solid-solid geologic interfaces. Furthermore, this method can be applied to RF's made from real teleseismic data. A particularly interesting set of such RF data is that produced by *Lewis et al.,* [2001]**,** from a set of passive teleseismic data recorded at a temporary array that extended across the Peninsular Ranges and Gulf Extensional Province in Baja California, México at about 31˚ north latitude.

A staggered-grid finite-difference (FD) technique (2nd order in time, 4th order in space) for the numerical simulation of a seismic wavefield propagating though a 3D elastic medium has been used [e.g., *Graves*, 1996]. This technique utilizes the discrete elastodynamic formulation of the full wave equation [e.g., *Madariaga*, 1976; *Virieux*, 1984, 1986; *Levander*, 1988] which enables modeling of the complete P-SV-SH seismic wavefield. This is important because of the need to accurately compute the magnitude of mode conversions at geologic interfaces [*Larsen and Grieger,* 1999], and is especially important for those where the combination of the angle of wavefield incidence and the geometry of the interface(s) produce a displacement field with a strong 3D component. In the past, a limitation of this type of seismic modeling was that it was very computationally expensive. However, the increase in availability of computers with enough speed and memory to run sufficiently large 3D FD seismic wave propagation experiments has eased this limitation.

Regional variations in crustal thickness in southern California and northern Baja California have been reported in several receiver function studies [e.g., *Ichinose et al*., 1996; *Zhu and Kanamori*, 2000; *Lewis, et al*., 2000, 2001]. These studies report that the Moho is shallow and roughly flat under the Salton trough and the northern Gulf of California. It then dips steeply westward reaching its greatest depth under the western Peninsular Ranges Batholith (PRB). Continuing westward the Moho gradually rises to intermediate depth near the Pacific coast and then becomes shallow and relatively flat once again offshore under the Inner California Borderland. Knowledge of Moho topography is important to seismic hazard and risk analysis because it strongly affects the propagation of seismic waves trapped within the crust and can directly influence the magnitude of strong ground motion at certain critical distances from large Earthquakes [*Zhu and Kanamori*, 2000].

It is significant that the Moho under the eastern PRB fails to correlate to the topography of the batholith [*Ichinose et al.*, 1996; *Lewis et al.*, 2000, 2001]. This implies that mechanisms other than an Airy root provide support for the eastern PRB. Late Miocene and early Pliocene extension and the opening of the Gulf of California may have influenced this configuration. In contrast the Moho underlying most of the Basin and Range Province is relatively flat even though this region underwent considerable extension during the Miocene [*McCarthy and Parsons*, 1994]. The lack of an Airy root has also been reported for the southern Sierra Nevada batholith (SNB) and central Transverse Ranges (CTR) [*Jones, Kanamori, and Roecker*, 1994; *Zhu and Kanamori*, 2000]. Because the PRB, CTR, and SNB are believed to be segments (along with the Salinian block) of the same continuous Mesozoic volcanic arc, and they share the same type of anomalous structure, it is possible this structure is the result of, or is linked to a common tectonic origin.

The homogeneous elastodynamic wave equation is the basis of this implementation. To facilitate the solution by finite differences the equation of motion is formulated into a first-order set of differential equations (first-order hyperbolic system) by differentiating and then substituting the time-differentiated displacements with the velocity components. The vertical component of the homogeneous elastodynamic wave equation is:

$$\partial_t v_z = \tfrac{1}{\rho}\left(\partial_x \tau_{xz} + \partial_y \tau_{yz} + \partial_z \tau_{zz}\right) \quad (1)$$

where v is the velocity, τ the components of the stress tensor, ρ is the density, and the symbols ∂_x, ∂_y, ∂_z, ∂_t, represent the differential operators. The time derivatives of the stresses are:

$$\begin{aligned} \partial_t \tau_{zz} &= (\lambda + 2\mu)\partial_z v_z + \lambda(\partial_x v_x + \partial_y v_y) \\ \partial_t \tau_{xz} &= \mu(\partial_z v_x + \partial_x v_z) \qquad (2) \\ \partial_t \tau_{yz} &= \mu(\partial_z v_y + \partial_y v_z) \end{aligned}$$

where λ and μ are the Lame coefficients.

A plane wave source for modeling teleseismic body waves is assumed because the distance between the source and receiver is large compared to the dimensions of the model. To implement the plane wave source the nodes of a planer region of the 3D model are excited using the inhomogeneous form of the elastodynamic wave equation. A term equivalent to a body force is added to the components of the seismic wave velocity. Here the vertical component includes the body force term, f_z.

$$\partial_t v_z = \tfrac{1}{\rho}\left(\partial_x \tau_{xz} + \partial_y \tau_{yz} + \partial_z \tau_{zz} + f_z\right) \quad (3)$$

Discretization of (3) by centered finite-differences (2nd order) in both time and space yields (4).

$$v_{z(i,j,k+1/2)}^{(n+1/2)} = v_{z(i,j,k+1/2)}^{(n-1/2)} + \left[\frac{\Delta t}{\rho}\left(D_x \tau_{xz} + D_y \tau_{yz} + D_z \tau_{zz} + f_z\right)\right]_{(i,j,k+1/2)}^{(n)} \quad (4)$$

Parenthesized subscripts are the spatial indices and parenthesized superscripts are the temporal indices, Δt is the time step, $\Delta x = \Delta y = \Delta z$ are the grid spacing, D_x, D_y, and D_z are the spatial differential operators, and $v_{z(i,j,k+1/2)}^{(n+1/2)}$ (5) represents the vertical velocity component at the point ($x=i\Delta x$, $y=j\Delta y$, $z=(k+½)\Delta z$) at time $t=(n+½)\Delta t$ (*Graves*, 1996). The addition of a body force equivalent term to the velocity calculation of the at time $t=(n+½)\Delta t$ is:

$$v_{z(i,j,k+1/2)}^{(n+1/2)} = v_{z(i,j,k+1/2)}^{(n+1/2)} + ss_{(\Delta t(n+1/2))} \quad (6)$$

where *SS(Δt(n+½))* is the scaled source term. Note: *v* is updated at (*n+1/2*)*Δt*, τ at (*n+1*)*Δt*, so the source is added at (*n+½*)*Δt*. The oblique plane wave source has been implemented with the source term partitioned between the vertical (z) and horizontal (x) components.

Synthetic seismograms have been produced for various geometries representing Moho structure beneath northern Baja California, Mexico. The final step will be to process these seismograms using a time domain deconvolution receiver function method [e.g. *Lewis, et al*. 2001]. A wavefield snapshot (Fig. 1) shows P and S components (via wavefield decomposition) of an oblique plane wave encountering a lower velocity dipping granitic layer over a mantle half space. This model shows a 25° west dipping Moho transitioning from a depth of 40.5km up to 18km. This is the estimate of average Moho dip given by *Lewis, et al*., 2001.

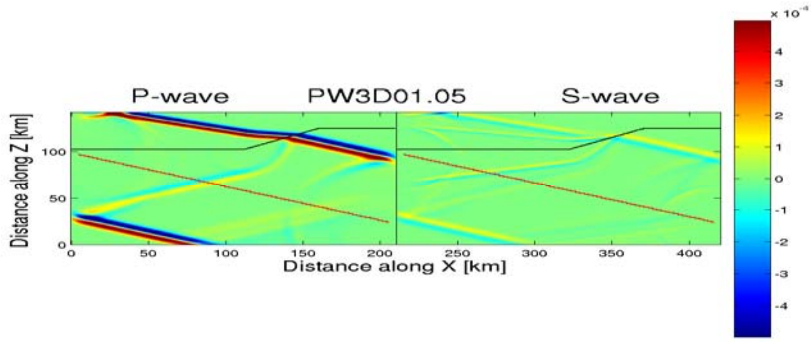

Figure 1. Wavefield snapshot (XZ plane) centered on the Y (N/S) axis. The P wavefield is shown in the left hand frame, S in the right. The red line is the source plane location and the black line is the Moho.

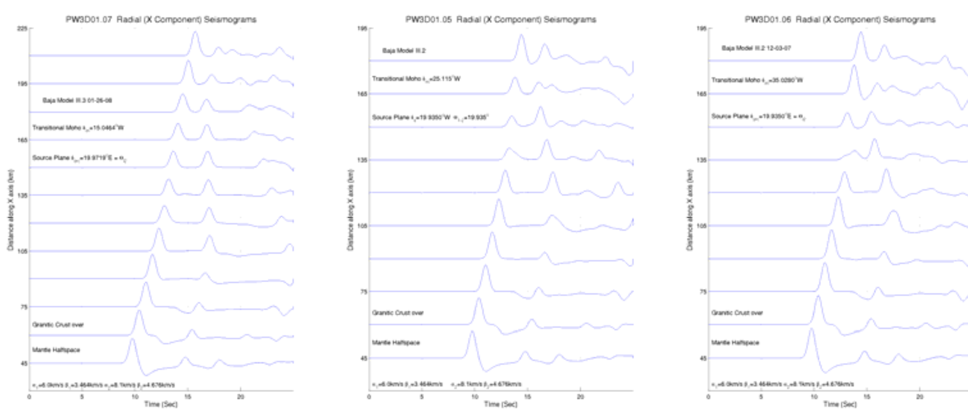

Figure 2. Radial seismograms for 3 different west dipping transitional Baja Moho models with dips of approximately 15˚, 25˚, and 35˚ respectively. The first arrival is P and second is the Ps converted phase. The same ray parameter was used in each simulation.

References

Ammon, C. J., G. E. Randall, and G. Zandt, On the nonuniqueness of receiver function inversions, *J. Geophys. Res.*, *95*, 15,303-15,318, 1990.

Ammon, C. J., The isolation of receiver effects from teleseismic P waveforms, *Bull. Seism. Soc. Am.*, *81*, 2504-2510, December 1991.

Ammon, C. J., Receiver function overview, *Penn State Faculty home page, Research notes*, 2003 http://www.eas.slu.edu/People/CJAmmon/HTML/RftnDocs/rftn01.html

Graves, R. W., Simulating seismic wave propagation in 3D elastic media using staggered-grid finite differences, *Bull. Seism. Soc. Am., 86*, 1091-1106, 1996.

Ichinose, G. A., S. Day, H. Magistrale, T. Prush, F. Vernon, and A. Edelaman, Crustal thickness variations beneath the Peninsular Ranges, southern California, *Geophys. Res. Lett., 23*, 3095-3098, 1996.

Jones, C. H., H. Kanamori, and S. W. Roecker, Missing roots and mantle "drips": Regional P_n and teleseismic arrival times in the southern Sierra Nevada and vicinity, California, *J. Geophys. Res., 99*, 4567-4601, 1994.

Jones, C. H., and R. A. Phinney, Seismic structure of the lithosphere from teleseismic converted arrivals at small arrays in the southern Sierra Nevada and vicinity, California, *J. Geophys. Res., 103*, 10,065-10,090, 1998.

Langston, C. A., Structure under Mount Rainier, Washington, inferred from teleseismic body waves, *J. Geophys. Res*., 84, 4749-4762, 1979.

Langston, C. A., and J. K. Hammer, The vertical component P-wave receiver function, *Bull. Seism. Soc. Am., 91*, 1091-1106, 2001.

Larsen, S. and J. Grieger, Elastic modeling initiative, Part III: 3-D computational modeling, 1998 Society of Exploration Geophysicists, New Orleans, LA, September 13-18, 1998.

Lay, T., and T. C. Wallace, *Modern Global Seismology*, 521 pp., Academic Press, 1995.

Levander, A. R., Fourth-order finite-difference P-SV seismograms, *Geophysics, 53*, 1425-1436, 1988.

Lewis, J., S. M. Day, H. Magistrale, F. Vernon, Regional crustal thickness variations of the Peninsular Ranges, southern California, *Geology*, *28*, 303-306, 2000.

Lewis, J., S. M. Day, H. Magistrale, R. R. Castro, L. Astiz, C., Rebollar, J. Eakins, F. Vernon, and J. N. Brune, Crustal thickness of the Peninsular Ranges and Gulf Extensional Province in the Californias, *J. Geophys. Res*., *106*, 13599-13611, 2001.

Madariaga, R., Dynamics of an expanding circular fault, *Bull. Seism. Soc. Am., 66*, 163-182, 1976.

McCarthy, J., and T. Parsons, Insights into the kinematic Cenozoic evolution of the Basin and Range-Colorado Plateau transition from coincident seismic refraction and reflection data, *Geo. Soc. Am. Bull., 106*, 747-759, 1994.

Owens, T. J., G. Zandt, and S. R. Taylor, Seismic evidence for an ancient rift beneath the Cumberland Plateau, Tennessee: a detailed analysis of broadband teleseismic P waveforms, *J. Geophys. Res., 89*, 7783-7795, 1984.

Reading, A. M.; Kennett, B. L. N., Lithospheric structure of the Pilbara Craton, Capricorn Orogen and northern Yilgarn Craton, Western Australia, from teleseismic receiver functions. *Australian Journal of Earth Sciences, 50,* 439-445, 2003.

Stein, S., and M. Wysession, *An Introduction to Seismology, Earthquakes, and Earth Structure*, 498 pp., Blackwell Publishing Ltd., 2003.

Virieux, J., SH wave propagation in heterogeneous media: velocity-stress finite-difference method, *Geophysics, 49*, 1933-1957, 1984.

Virieux, J., P-SV wave propagation in heterogeneous media: velocity-stress finite-difference method, *Geophysics, 51*, 889-901, 1986.

Zhang, J., and C. A. Langston, Dipping structure under Dourbes, Belgium, determined by receiver function modeling and inversion, *Bull. Seism. Soc. Am., 85*, 254-268, 1995.

Zhu, L., and H. Kanamori, Moho depth variation in southern California from teleseismic receiver functions, *J. Geophys. Res., 105*, 2969-2980, 2000.